

New Supporting Evidence for the Overdensity of Galaxies around the Radio-Loud Quasar SDSS J0836+0054 at $z = 5.8$

Masaru AJIKI,¹ Yoshiaki TANIGUCHI,¹ Takashi MURAYAMA,¹
Yasuhiro SHIOYA,¹ Tohru NAGAO,^{2,3} Shunji S. SASAKI,¹ Yuichiro HATAKEYAMA,¹ Taichi MORIOKA,¹
Asuka YOKOUCHI,¹ Mari I. TAKAHASHI,¹ and Osamu KOIZUMI¹

¹*Astronomical Institute, Graduate School of Science, Tohoku University,
Aramaki, Aoba-ku, Sendai 980-8578*

²*INAF — Osservatorio Astrofisico di Arcetri,
Largo Enrico Fermi 5, 50125 Firenze, Italy*

³*National Astronomical Observatory,
Osawa, Mitaka, Tokyo 181-8588, Japan*

(Received 2006 January 11; accepted 2006 March 10)

Abstract

Recently, Zheng et al. (2005) found evidence for an overdensity of galaxies around a radio-loud quasar, SDSS J0836+0054, at $z = 5.8$ (a five arcmin² region). We have examined our deep optical imaging data (B , V , r' , i' , z' , and $NB816$) taken with the Suprime-Cam on the Subaru Telescope. The $NB816$ narrow-band filter ($\lambda_c = 815$ nm and $\Delta\lambda = 12$ nm) is suitable for searching for Ly α emitters at $z \approx 5.7$. We have found a new strong Ly α emitter at $z \approx 5.7$ close to object B identified by Zheng et al. Further, the non detection of the nine objects selected by Zheng et al. (2005) in our B , V , and r' images provides supporting evidence that they are high- z objects.

Key words: cosmology: observations — cosmology: early universe — galaxies: formation — galaxies: evolution

1. Introduction

The growth of large scale structure in the early universe is one of the important issues in the understanding of structure formation in context of hierarchical models of galaxy formation (e.g., Press & Schechter 1974; Peebles 1993). Since the discovery of an overdensity region (or a proto cluster) of galaxies in a deep survey field, SSA22 (Steidel et al. 2000; see also Matsuda et al. 2005), deep surveys of such overdensity regions have been intensively made, leading to findings of clustering of galaxies at $z \sim 5 - 6$ (Shimasaku et al. 2003; Ouchi et al. 2005; Wang et al. 2005; Malhotra et al. 2005).

In addition to these findings, deep surveys for sky areas surrounding high-redshift active galactic nuclei such as radio galaxies and quasars also succeeded in finding overdensity regions; e.g., (1) a radio galaxy, TN1338–1942 at $z = 4.1$ (Venemans et al. 2002; Miley et al. 2004), (2) a radio galaxy, TN 0924–2201 at $z = 5.2$ (Venemans et al. 2004; Overzier et al. 2005), (3) a quasar, SDSS J1030+0524 at $z = 6.28$ (Stiavelli et al. 2005), and (4) a radio-loud quasar, SDSS J0836+0054 at $z = 5.8$ (Zheng et al. 2005). Among these interesting overdensity regions, we present our deep survey for Ly α emitters (hereafter LAEs) in the Zheng et al.'s field surrounding the radio-loud quasar SDSS J0836+0054 at $z = 5.8$ because this quasar is one of our target high- z quasars (Ajiki 2006; Ajiki et al. 2006 in preparation).

As demonstrated in previous optical narrow-band imag-

ing surveys, a redshift range between $z = 5.6$ and 5.8 is one of favorable windows for any ground-based telescopes because OH airglow emission lines are fairly weak at $\lambda \sim 815$ nm, corresponding to a Ly α redshift of $z \approx 5.7$ (e.g., Hu et al. 1999, 2004; Rhoads & Malhotra 2001; Rhoads et al. 2003; see for a review Taniguchi et al. 2003b). Using the prime focus camera, Suprime-Cam, on the 8.2m Subaru Telescope, we have been promoting our narrow-band imaging survey for LAEs in selected sky areas in which SDSS high- z quasars at $z \sim 6$ are found (Fan et al. 2000, 2001, 2002, 2003); see for our earlier results, Ajiki et al. (2002, 2003, 2004), Taniguchi et al. (2003a).

We adopt a flat universe with $\Omega_{\text{matter}} = 0.3$, $\Omega_{\Lambda} = 0.7$, and $H_0 = 70$ km s⁻¹ Mpc⁻¹. Throughout this paper, magnitudes are given in the AB system.

2. Observations and Data Reduction

2.1. Observations

We have carried out very deep optical imaging in the field surrounding the quasar SDSS J0836+0054 at redshift 5.8 (Fan et al. 2001), using the Suprime-Cam (Miyazaki et al. 2002) on the 8.2 m Subaru Telescope (Kaifu et al. 2000; Iye et al. 2004) on Mauna Kea. The Suprime-Cam consists of ten $2k \times 4k$ CCD chips and provides a very wide field of view, $34' \times 27'$ ($0''.2$ pixel⁻¹). In this survey, we used broad-passband filters, B , V , r' , i' , and z' . We also used a narrow-passband filter, $NB816$, centered on 815 nm with a passband of $\Delta\lambda_{\text{FWHM}} = 12$ nm; the wave-

length corresponds to a redshift of 5.65 – 5.75 for Ly α emission. All observations were done under photometric conditions, and the seeing was between 0.''7 and 1.''1 during our observing runs made in 2004 (see for details Ajiki 2006; Ajiki et al. 2006 in preparation). The individual CCD data were reduced and combined using IMCAT by the standard process.

2.2. Photometry

We performed photometry of the objects A – G found by Zheng et al. (2005). The photometry is performed with a 1'' diameter aperture for each band image of which image sizes of the stars have a FWHM of 1.''15. The limiting magnitudes are $B = 28.4$, $V = 28.6$, $r' = 28.1$, $i' = 27.9$, $z' = 27.2$, and $NB816 = 27.3$ for a 2σ detection with a 1'' diameter aperture. The reason for the use of a 1'' diameter aperture is to exclude possible light contamination of neighbor objects around each target object from A to G. Note that the light contamination in the object F could not be excluded completely even when we use the above small aperture. The results of the photometry are summarized in Table 1. Since all of objects except for the object F in Table 1 are not detected in the B , V , and r' images above 1σ level (i.e., $B = 29.1$, $V = 29.3$, and $r' = 28.8$), we give only i' , z' , and $NB816$ magnitudes in this table. The images of the objects are shown in Figure 1.

3. Results and Discussion

3.1. A New Ly α Emitter at $z = 5.7$

During the inspection of the sky area around SDSS J0836+0054, we find a new LAE candidate close to object B (see the 2nd row of Figure 1). It is detected in $NB816$ while not detected in the broad bands. We refer this object as to B'. This object is seen at 1.''12 NE from object B.

If the excess in $NB816$ is due to Ly α emission, the redshift of B' is 5.7 ± 0.05 being very similar to the photometric redshift of B, $z_{\text{ph}}(\text{line}) = 5.8$ (see section 3.3). The angular separation (1.''12) between B and B' corresponds to a projected distance of 6.5 kpc at $z = 5.7$. The angular distance of B' from the quasar is 74.''9. This corresponds to a projected separation of 440 kpc.

It is likely that these two objects are in a common dark matter halo (e.g., Hamana et al. 2004). This system is another interacting system such as the three (or two) components of object C (Zheng et al. 2005) in this overdensity region. We estimate the Ly α luminosity of this object, $L(\text{Ly}\alpha) = 8.6 \times 10^{42}$ ergs s $^{-1}$, from the $NB816$ flux in the 2'' diameter aperture [$NB816(2'') = 24.8$]. This luminosity is typical among the LAEs found at $z = 5.7$ (e.g., Ajiki et al. 2003; Hu et al. 2004).

3.2. Narrow-band photometry of Zheng et al.'s Objects

Non detection of the nine objects selected by Zheng et al. (2005) in our B , V , and r' images provides supporting evidence that they are high- z objects. Since we have $NB816$ photometry in addition to the broad bands, we can derive precise information of redshifts using the

narrow-band data. For instance, a LAE at $z = 5.65 - 5.75$ shows $NB816$ excess to the z' band while $NB816$ dropout objects are considered to be at $z > 5.8$ (Shioya et al. 2005b).

As shown in Table 1 objects A and F were detected 2.2σ and 5σ significance in the narrow-band image, respectively. Note that the object F is apparently affected by the foreground object seen in the north. However, since one can identify their $NB816$ counterparts to the z' image (Fig. 1), we consider that detection of A and F is real. They are not $NB816$ dropout objects and thus their redshifts are probably not greater than 5.8. Since Zheng et al. (2005) estimated their photometric redshifts of 5.7 – 5.8, at least the objects A and F may be associated closed to the quasar redshift of 5.8.

For the remaining seven objects, $NB816$ was not detected above 2σ level. However, we cannot conclude if their redshifts are greater than 5.8 or not here because the limiting magnitude of $NB816$ is not deep enough compared to each z' magnitude. Photometric redshift technique with $NB816$ and the broad bands provides possible redshifts of them from our photometric data (section 3.3).

3.3. Photometric Redshifts of Zheng et al.'s Objects

Zheng et al. (2005) estimated photometric redshifts for the nine objects A – G using the Bayesian photometric redshift technique (Benítez 2000) based on their HST ACS data, i_{775} and z_{850} . Since we have $NB816$ photometry for the nine objects, it is worthwhile estimating their photometric redshifts because this trial gives an independent test for Zheng et al.'s (2005) results. Note that our photometry is made with a 1'' aperture and thus the magnitudes given in Table 1 are not total magnitudes. Therefore, we use only our photometric data of i' , z' , and $NB816$.

Using the maximum likelihood described in Shioya et al. (2005a; see for our SED templates, Nagao et al. 2004), we estimate a most probable photometric redshift for each object. In this procedure, we adopt an allowed redshift of between $z = 0$ and $z = 7$ with a redshift bin of $\Delta z = 0.01$. Our photo- z analysis suggests that objects A, B, and F may be low- z sources; $z_{\text{ph}} \sim 1.8$ for A, $z_{\text{ph}} \sim 1.2$ for B, and $z_{\text{ph}} \sim 0.24$ for F. These are due to that our $i' - z'$ colors of these three objects are slightly bluer than those ($i_{775} - z_{850}$) of Zheng et al. (2005). However, the photometric accuracy in Zheng et al. (2005) in their i_{775} and z_{850} seems to be better than ours in i' and z' . We, therefore, adopt a z_{ph} whose likelihood is high at high- z domain.

We do not know that the nine objects are always strong LAEs. Therefore, we estimate two kinds of photometric redshifts; one is $z_{\text{ph}}(\text{no line})$ in which there is no Ly α emission, and $z_{\text{ph}}(\text{line})$ in which the effect of Ly α emission is taken into account. In Table 1, we give our results together with the Bayesian photometric redshifts (z_{BP}) obtained by Zheng et al. (2005).

We find that our estimates are nearly consistent with those by Zheng et al. (2005). However, as for the three components of object C (C, C2, and C3), our results are

slightly different from theirs. This difference may be attributed to that our photometry is affected by neighbor objects to some extent because our image quality is not as good as HST ACS data. Since it is likely that most galaxies at $z \sim 6$ show the Ly α emission (e.g., Taniguchi et al. 2005 and references therein), we consider that the reliability of $z_{\text{ph}}(\text{line})$ could be better than that of $z_{\text{ph}}(\text{no line})$. If this is the case, the seven objects (A, B, C3, D, E, F, and G) have redshifts between $z = 5.8$ and $z = 6.0$. Although spectroscopic follow-up observations are necessary, we may conclude that most of the objects found by Zheng et al. (2005) and one LAE at $z_{\text{ph}} \simeq 5.7$ found in this study are associated with SDSS J0836+0054.

3.4. The Overdensity of Galaxies around SDSS J0836+0054

Based on their deep HST images, Zheng et al. (2005) found five i_{775} faint objects and two i_{775} dropout in a five arcmin² sky area around SDSS J0836+0054. Comparing their finding with those obtained with GOODS (Giavalisco et al. 2004; Dickinson et al. 2004; Bouwens et al. 2005), they suggested that this region shows an overdensity of galaxies by a factor of six. Although one cannot rule out the effect of the cosmic variance, other deep surveys also find such overdensity regions at $z \sim 6$ (e.g., Ouchi et al. 2005; Wang et al. 2005; Malhotra et al. 2005). Our new finding of the LAE at $z = 5.7$ also provides additional supporting evidence for the overdensity in this region. Further investigations of probable overdensity regions in blank deep survey fields and targeted fields around high- z radio galaxies and quasars will be important to improve our understanding of the formation and evolution of large scale structure in the early universe.

We would like to thank the Subaru Telescope staff for their invaluable help. We would also thank to the referee, Bram P. Venemans, for his useful comments and suggestions. This work was financially supported in part by JSPS (Nos. 15340059, and 17253001). MA, SSS, and TN are JSPS fellows.

References

- Ajiki, M. 2006, PhD Thesis, Tohoku University
 Ajiki, M., et al. 2002, ApJ, 576, L25
 Ajiki, M., et al. 2003, AJ, 126, 2091
 Ajiki, M., et al. 2004, PASJ, 56, 597
 Benítez, N. 2000, ApJ, 536, 571
 Bouwens, R. J., Illingworth, G. D., Blakeslee, J. P., & Franx, M. 2005, ApJ, in press (astro-ph/0509641)
 Bruzual, G., & Charlot, S. 2003, MNRAS, 344, 1000
 Calzetti, D., Armus, L., Bohlin, R. C., Kinney, A. L., Koorneef, J., Storch-Bergmann, T. 2000, ApJ, 533, 682
 Dickinson, M., et al. 2004, ApJ, 600, L99
 Fan, X., et al. 2000, AJ, 120, 1167
 Fan, X., et al. 2001, AJ, 121, 54
 Fan, X., et al. 2002, AJ, 122, 2833
 Fan, X., et al. 2003, AJ, 125, 1649
 Fioc, M., & Rocca-Volmerange, B. 1997, A&A, 326, 950
 Giavalisco, M., et al. 2004, ApJ, 600, L103
 Hamana, T., Ouchi, M., Shimasaku, K., Kayo, I., & Suto, Y. 2004, MNRAS, 347, 813
 Hu, E. M., McMahon, R. G., & Cowie, L. L. 1999, ApJ, 522, L9
 Hu, E. M., et al. 2004, AJ, 127, 563
 Iye, M., et al. 2004, PASJ, 56, 381
 Kaifu, N., et al. 2000, PASJ, 52, 1
 Leitherer, C., & Heckman T. M. 1995, ApJS, 96, 9
 Madau, P., Ferguson, H. C., Dickinson, M. E., Giavalisco, M., Steidel, C. C., & Fruchter, A. 1996, MNRAS, 283, 1388
 Malhotra, S., Wang, J. X., Rhoads, J. E., Heckman, T. M., & Norman, C. A. 2003, ApJ, 585, L25
 Matsuda, Y., et al. 2005, ApJ, 634, L125
 Miley, G., et al. 2004, Nature, 427, 47
 Miyazaki, S., et al. 2002, PASJ, 54, 833
 Nagao, T., et al. 2004, ApJ, 613, L9
 Ouchi, M., et al. 2005, ApJ, 620, L1
 Overzier, R., et al. 2005, ApJ, in press (astro-ph/0509308)
 Peebles, P. J. E. 1993, Principles of Physical Cosmology (Princeton University Press)
 Press, W. H., & Schechter, P. 1974, ApJ, 187, 425
 Rhoads, J. E., & Malhotra, S. 2001, ApJ, 563, L5
 Rhoads, J. E., et al. 2003, AJ, 125, 1006
 Shimasaku, K., et al. 2003, ApJ, 586, L111
 Shioya, Y., et al. 2005a, PASJ, 57, 287
 Shioya, Y., et al. 2005b, PASJ, 57, 569
 Steidel, C. C., Adelberger, K. L., Shapley, A. E., Pettini, M., Dickinson, M., & Giavalisco, M. 2000, ApJ, 532, 170
 Stiavelli, M., et al. 2005, ApJ, 622, L1
 Taniguchi, Y., et al. 2003a, ApJ, 585, L97
 Taniguchi, Y., Shioya, Y., Fujita, S. S., Nagao, T., Murayama, T., & Ajiki, M. 2003b, JKAS, 36, 123; Erratum JKAS, 36, 283
 Taniguchi, Y., et al. 2005, PASJ, 57, 165
 Venemans, B. P., et al. 2002, ApJ, 569, L11
 Venemans, B. P., et al. 2004, A&A, 424, L17
 Zheng, W., et al. 2005, ApJ, in press (astro-ph/0511734)

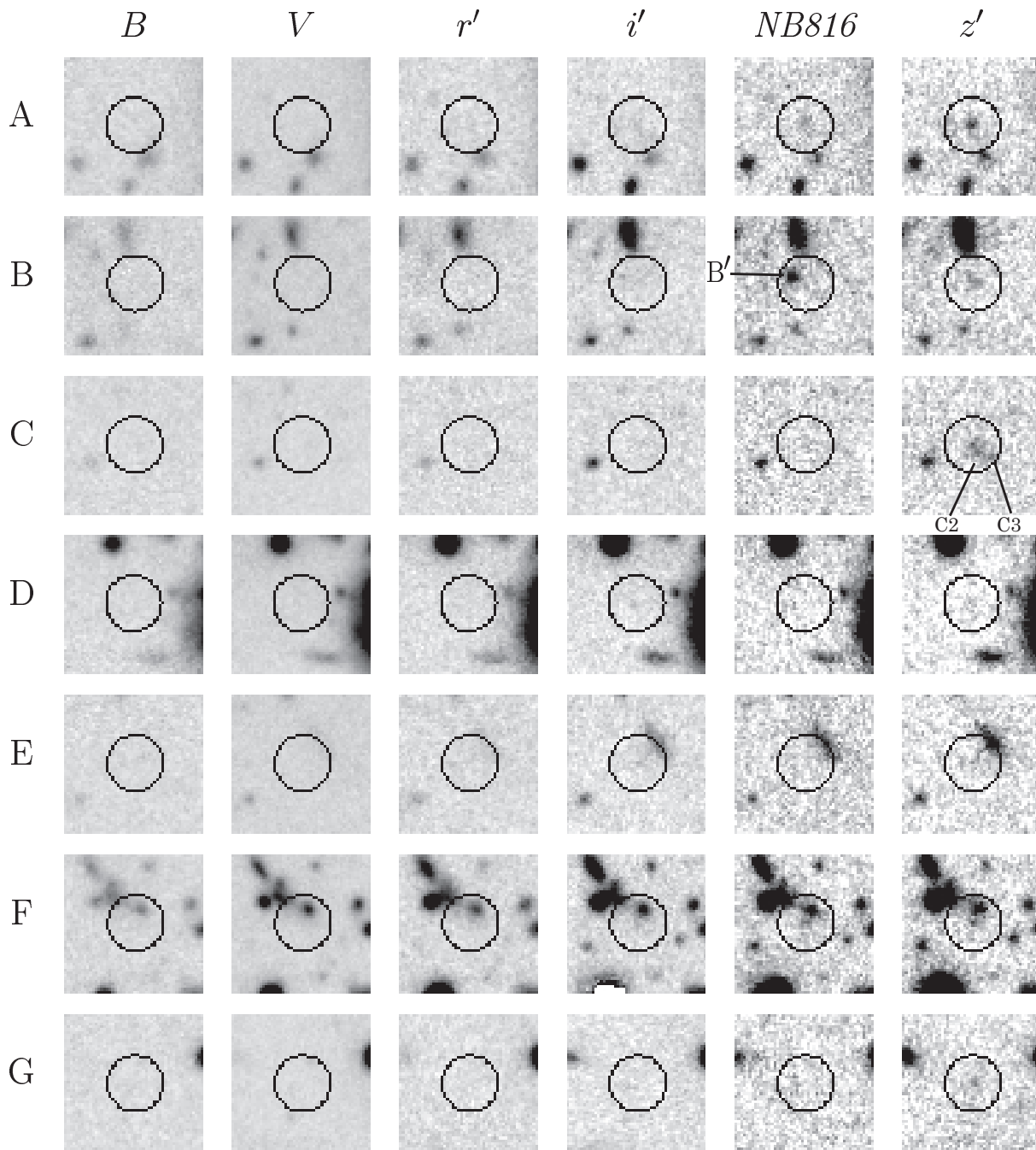


Fig. 1. Broad-band and $NB816$ images of the object A – G found by Zheng et al. (2005). The LAE newly found in our study, B' is shown in the $NB816$ image of object B. Each box is $10''$ on a side (north is up and east is right). Each circle has $2''$ radius.

Table 1. Photometric properties of the *i*-dropout and *i*-faint objects

Z05*	i'^{\dagger}	z'^{\dagger}	NB816 [†]	z_{BP}^{\ddagger}	$z_{ph}(\text{no line})^{\S}$	$z_{ph}(\text{line})^{\parallel}$
A	$28.0^{+0.9}_{-0.5}$	$26.4^{+0.3}_{-0.2}$	$27.2^{+0.7}_{-0.4}$	$5.8^{+1.4}_{-0.2}$	$5.66^{+1.26\#}_{-0.46}$	$5.72^{+1.13\#}_{-0.61}$
B	$28.4^{+1.7}_{-0.6}$	$27.1^{+0.6}_{-0.4}$	> 27.3	$5.9^{+1.0}_{-1.0}$	$5.68^{+1.26\#}_{-0.68}$	$5.77^{+1.08\#}_{-0.77}$
C	> 28.1	$26.6^{+0.4}_{-0.3}$	> 27.4	$5.9^{+1.1}_{-0.5}$	$6.59^{+0.41}_{-0.91}$	$6.73^{+0.20}_{-0.75}$
C2	> 28.2	$26.5^{+0.3}_{-0.2}$	> 27.8	$5.9^{+1.1}_{-1.5}$	$6.14^{+0.86}_{-0.32}$	$6.31^{+0.69}_{-0.38}$
C3	$28.5^{+2.1}_{-0.7}$	$26.9^{+0.5}_{-0.3}$	> 28.0	$7.0^{+0.0}_{-0.7}$	$5.74^{+1.26}_{-0.06}$	$5.78^{+1.21}_{-0.05}$
D	> 28.5	$27.8^{+2.6}_{-0.7}$	> 28.0	$5.8^{+1.2}_{-0.7}$	$6.98^{+0.02}_{-1.27}$	$6.01^{+0.99}_{-0.23}$
E	$28.0^{+0.9}_{-0.5}$	$27.4^{+1.0}_{-0.5}$	> 28.0	$5.2^{+1.7}_{-0.7}$	$5.72^{+1.28}_{-0.72}$	$5.81^{+0.21}_{-0.81}$
F**	$26.9^{+0.2}_{-0.2}$	$26.5^{+0.3}_{-0.3}$	$26.3^{+0.2}_{-0.2}$	$5.7^{+1.2}_{-0.7}$	$5.18^{+0.10\#}_{-0.18}$	$5.72^{+0.05\#}_{-0.54}$
G	> 28.2	$27.1^{+1.2}_{-0.4}$	> 27.8	$5.8^{+1.2}_{-0.8}$	$6.96^{+0.04}_{-1.27}$	$5.98^{+1.02}_{-0.16}$
B' ^{††}	$28.5^{+2.3}_{-0.7}$	> 27.4	$25.8^{+0.1}_{-0.1}$		$5.53^{+0.06}_{-0.20}$	$5.70^{+0.03}_{-0.05}$

*Object ID shown in Zheng et al. (2005)

[†]AB magnitude in a 1'' diameter. The total magnitude is expected to be $\gtrsim 1$ mag brighter.[‡]Bayesian photometric redshift given by Zheng et al. (2005).[§]Photometric redshift derived from the high- z peak of the likelihood in which there is no Ly α emission. The error shows 1 σ confidence level between $z = 5$ and 7.^{||}Photometric redshift derived from the high- z peak of the likelihood in which the effect of Ly α emission is taken into account. The error shows 1 σ confidence level between $z = 5$ and 7.[#]The highest peak of the likelihood appears at $z < 5$ (see text).

**Photometry appears to be affected by the foreground object.

^{††}LAE candidate at $z \approx 5.7$ found near object B.